Thermal X-ray radiation from hot polar cap in pulsars with drifting subpulses

Janusz Gil

J. Kepler Astronomical Institute
University of Zielona Góra, Poland

Collaborators:

G. Melikidze, B. Zhang, U. Geppert, F. Haberl

40 years after discovery of pulsars the actual mechanism of their coherent radio emission is still a mystery.

Drifting subpulses, which seem to be a common phenomenon in pulsar radiation, is also a puzzle.

„The mechanism for drifting subpulses cannot be very different from the mechanism of observed radio emission ...

...intrinsic property of radiation mechanism „

(Weltevrede, Edwards & Stappers 2006, AA 445; also Poster P10)

Drifting subpulses

Apparent drift-bands

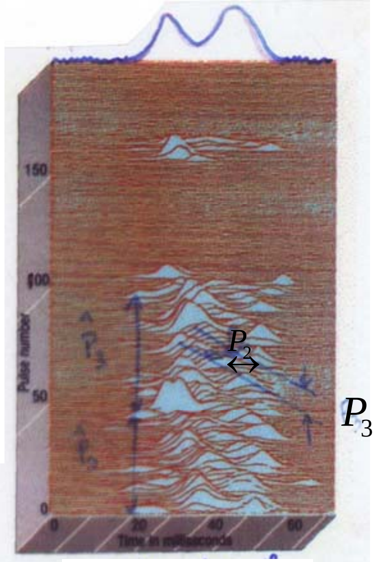

Subpulses in subsequent pulses arrive in phases determined by the apparent drift rate

$$D = P_2 / P_3$$

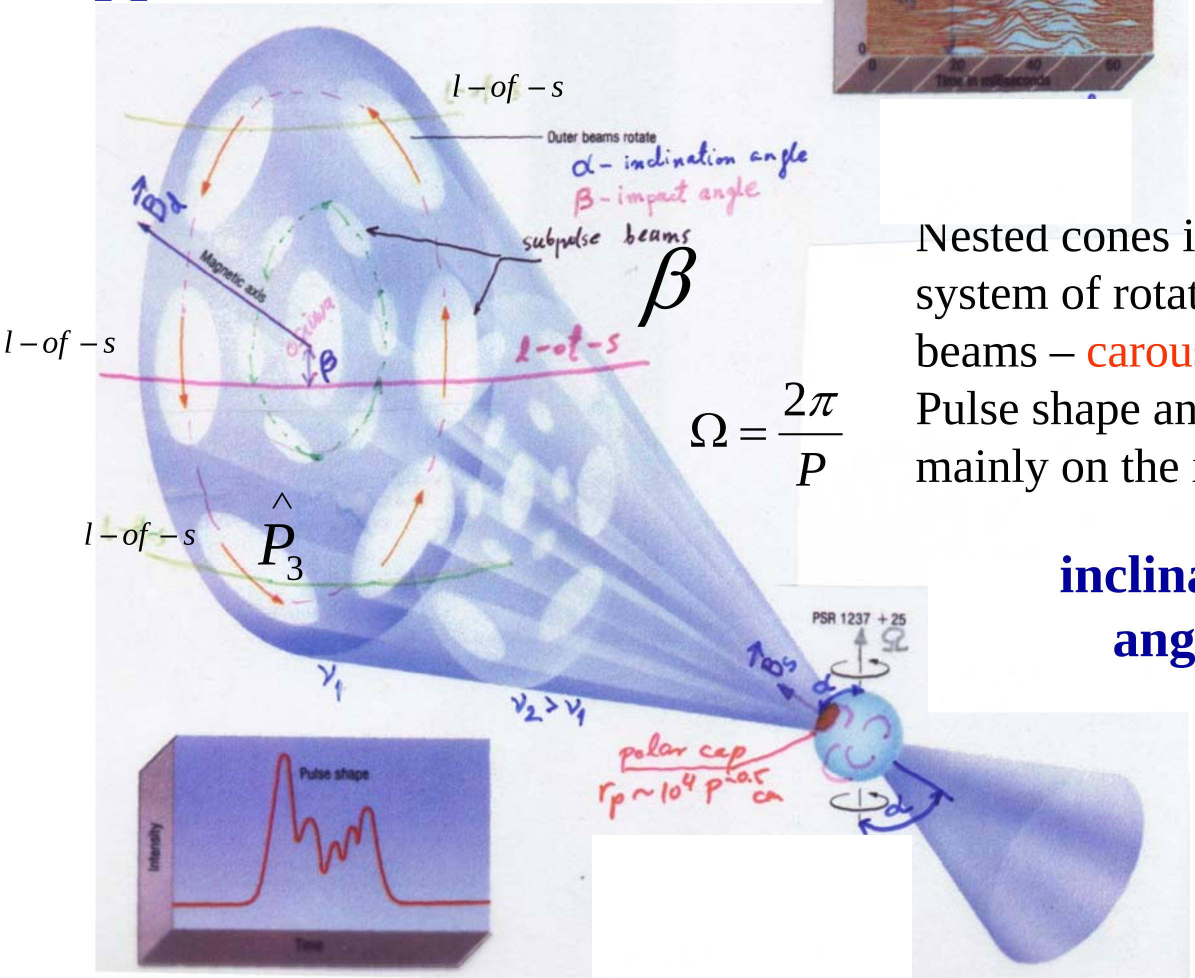

Nested cones induced by system of rotating subpulse beams – carousel model

Pulse shape and drift pattern depends mainly on the impact angle β

inclination angle α

Polar cap

$$r_{pc} = 1.45 \times 10^4 P^{-0.5} cm$$

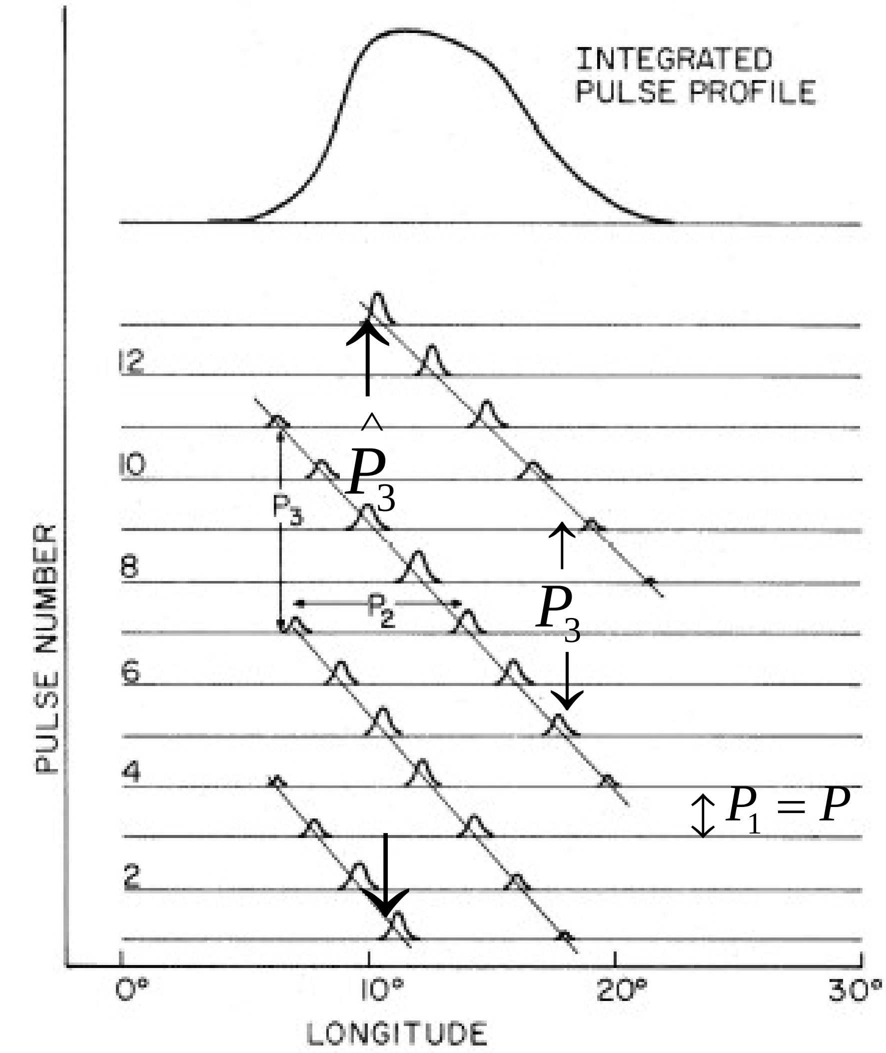

FIG. 5.—Schematic (after Backer 1973) of integrated pulse profile, arrival times of individual pulses, and definition of P_2, P_3 for those pulsars showing the "drifting subpulse" phenomenon. Arrival times of individual pulses are given in terms of a longitude for which 360° corresponds to the full pulsar period.

Ruderman & Sutherland 1975

$$P_1, P_2, P_3, \hat{P}_3$$

Apparent drift rate $D = P_2 / P_3$

P_3 **distance between driftbands in** P_1

Intrinsic drift rate $\hat{P}_3 = P_3 N$

N **number of rotating sub-beams**

$\hat{P}_3$ **distance between the same driftbands**

$\hat{P}_3$ **time interval to complete one rotation around the pole**

very difficult to measure, only 4 cases known !!!

PSR B0943+10

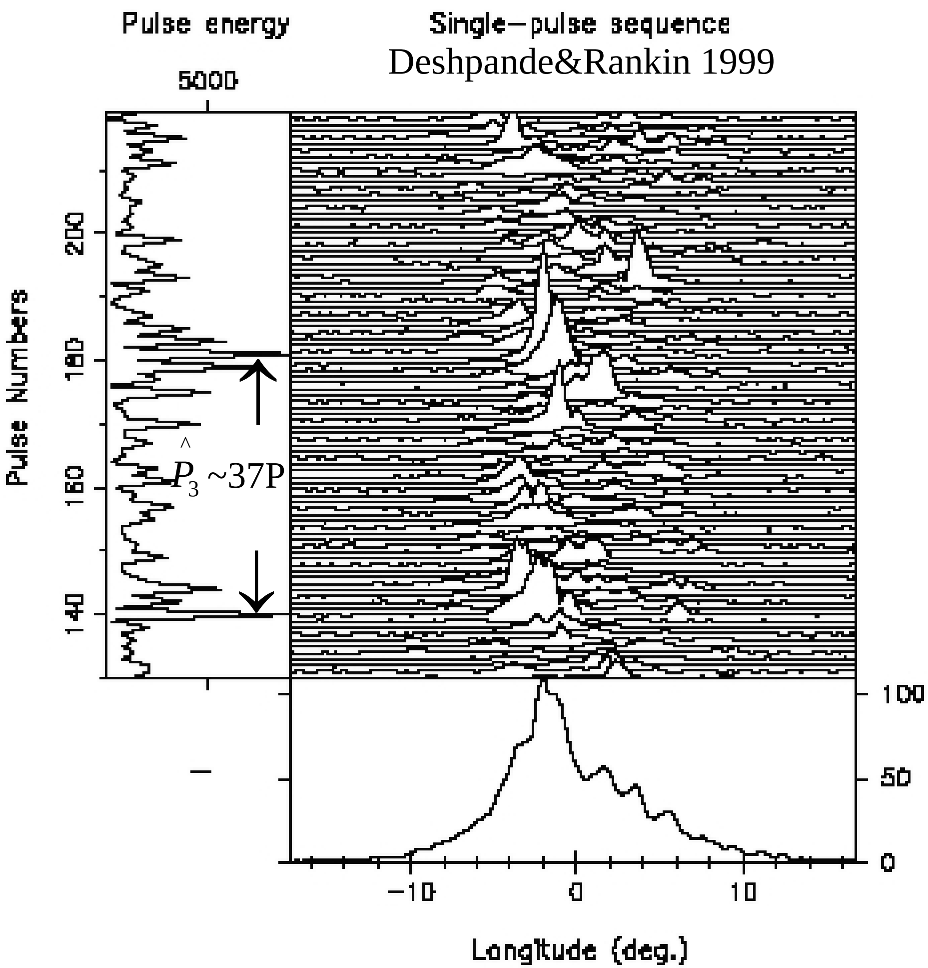

P=1.089 s

$P_3 = 1.87P$ primary

$P_3 = 2.15P$ aliased

$\hat{P}_3 = 37.35P$ **tertriary**

Number of sub-beams

$N = \hat{P}_3 / P_3 = 20$

Deshpande & Rankin 1999,2001
Asgekar & Deshpande 2001

Phased-resolved fluctuation spectrum

$$\hat{P}_3 = 37.35\,P = 41\text{s.}$$

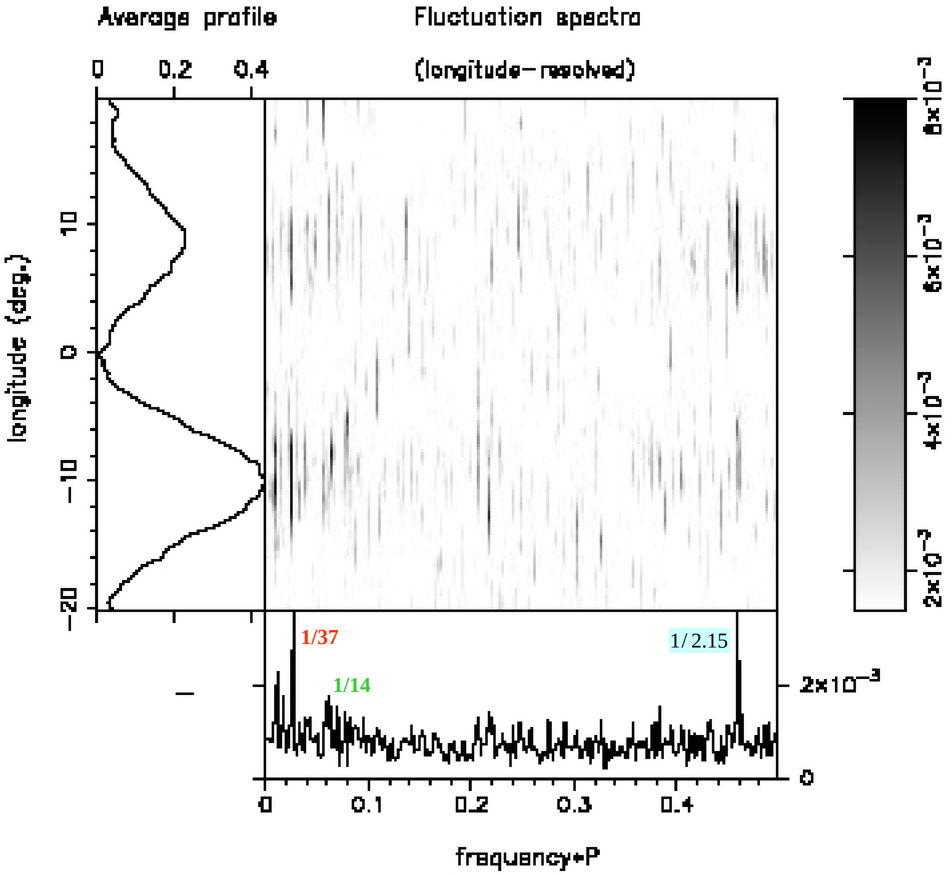

Spectral analysis fully consistent with „carousel model"
Sub-beams continue circulation around the beam axis beyond the pulse-window and reapear after the period needed to complete one full circulation around the magnetic axis

$$\frac{1/37.35}{1.86} = 20$$

B0943+10 Cartographic map of 20 subpulse beams „circulating" around the pole in about 37 pulsar periods

Deshpande & Rankin, 1999

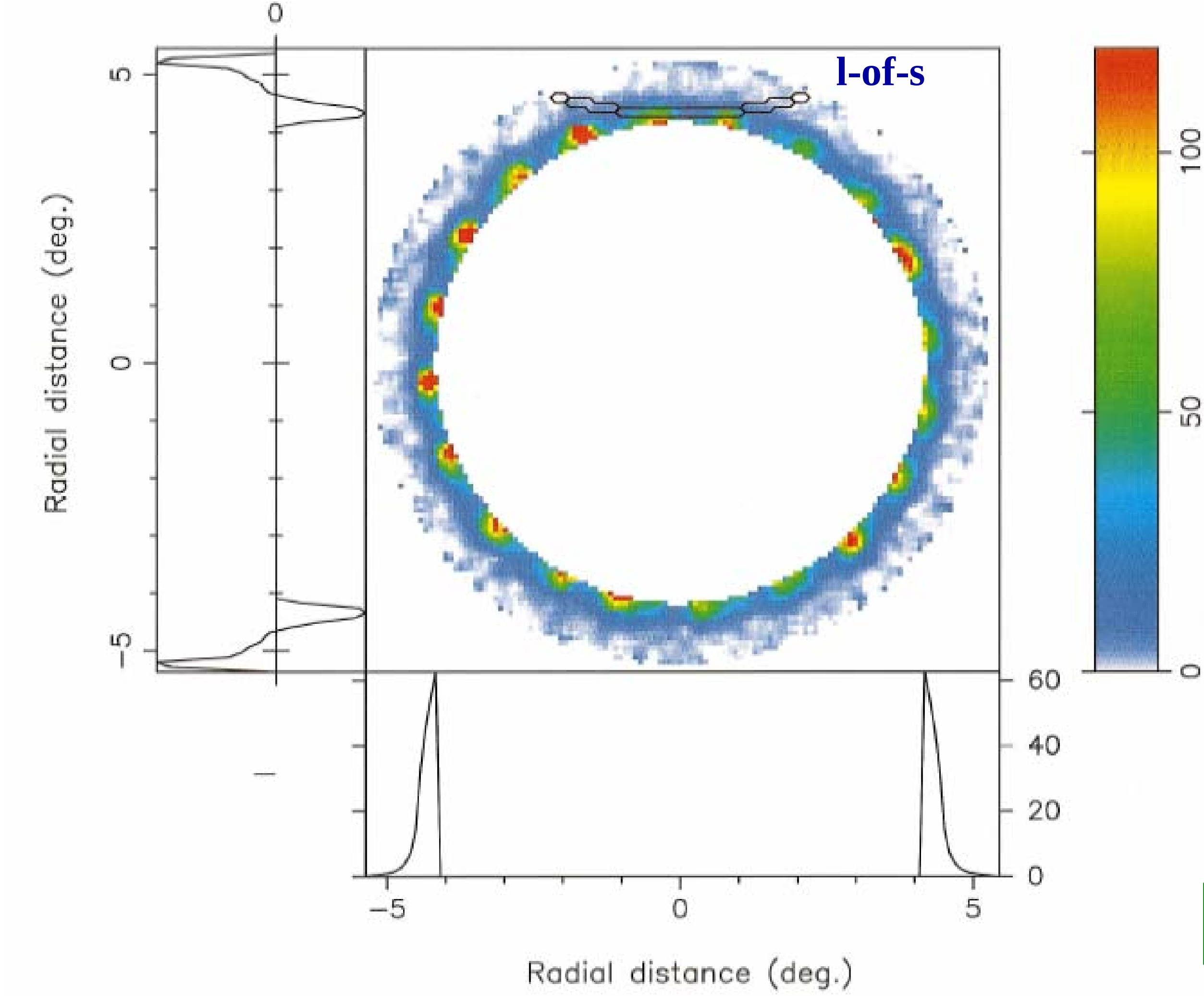

$P = 1.098$ s

$P_3 = 1.86\ P$

$\hat{P}_3 = 37.35\,P$

$N = \hat{P}_3 / P_3 = 20$

α, β *Pulsar geometry known*

(Intensity; pulse longitude and pulse number) →(Intensity; polar colatitude and azimuth)

Clear manifestation of subpulse sub-beams circulating around the magnetic axis

Natural mechanism of subpulse drift

$E \times B$

Ruderman & Sutherland 1975

$$\upsilon_{cor} = c(E_c \times B_s)/B^2 = cE_c/B_s \quad \Leftarrow \rho = \rho_{GJ}$$ corotation

$$if \quad E \neq E_c \quad then \quad \upsilon \neq \upsilon_{cor} \quad \Longleftarrow \rho \neq \rho_{GJ}$$ Polar Gap charge depletion

Non-corotation plasma lags behind pulsar rotation and drifts with respects the polar cap surface with velocity υ_{dr}

$$\boxed{\upsilon_{dr} = c(\Delta E \times B_s)/B^2 = cE_c/B_s}$$

ΔE Electric field associated with charge depletion $\Delta\rho = \rho_{GJ} - \rho$

If plasma has transversal structure (discharging spark filaments) then this inevitable

$\Delta E \times B$ **drift should be observed in the form of drifting subpulses**

Ruderman & Sutherland 1975

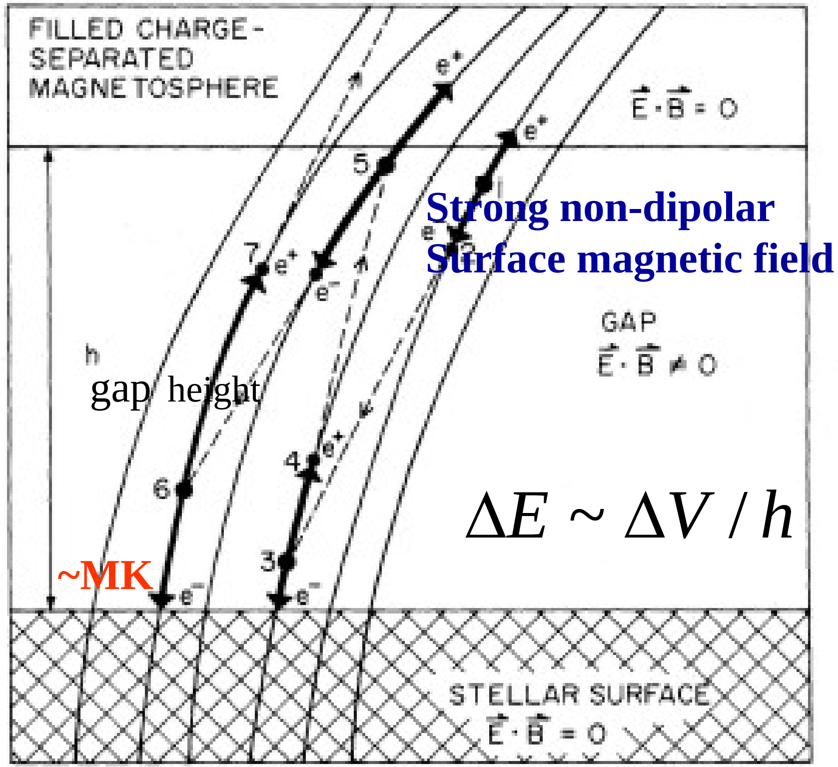

Within the acceleration region the spark generated positrons are moving towards the magnetosphere while back-flow of electrons bombard the polar cap surface and heat it to MK temperatures

Pure vacuum gap

Charge depletion maximum possible $\Delta\rho = \rho_{GJ}$

Very strong electric field ΔE

$\Delta E \times B$ **drift much too fast as compared with observations**

Polar cap heating too intense as compared with observations

Modification needed

Partialy Screened Gap (PSG) model

Cheng & Ruderman 1982; Gil, Melikidze & Geppert 2003

Electron-positron plasma created in sparks co-exists with thermionic flow caused by back-flow bombardment

$$\rho_{\pm} + \rho_{th} = \rho_{GJ}$$

Surface temperature of spark-heated polar cap

$$T_s \geq 10^6\ K \qquad T_s \leq T_i$$

$$T_i = \varepsilon / 30k = (7 \times 10^4\ K)(B_s / 10^{12}\ G)^{0.7}$$

Ion critical temperature (Jones 1986)

above this T there is maximum thermionic flow from the PC surface with GJ density (SCLF)

$$\eta = 1 - \rho_{th} / \rho_{GJ} = 1 - \exp[30(1 - T_i / T_s)]$$

Screening factor

Spark-associated polar cap heating within partially screened gap model

$$\sigma T_s^{\ 4} = \gamma m_e c n$$

Back-flow bombardment

$$\gamma = e\Delta V / m_e c^2$$

$$\Delta V = \eta (2\pi / cP) B_s h^2$$

$$n = n_{GJ} - n_{th} = \eta n_{GJ}$$

Charge number density

Goldreich-Julian (co-rotational) charge number density

$$n_{GJ} = 1.4 \times 10^{11} (B_s / B_d)(\dot{P} / 10^{-15})^{0.5} P^{-0.5}\ cm^{-3}$$

Actual surface temperature of heated polar cap (2-4) MK

$$T_s = (2 \times 10^6\ K) P^{-0.25} (\dot{P} / 10^{-15})^{0.25} \eta^{0.5} (B_s / B_d)^{0.5} (h / 10^3 cm)^{0.5}$$

$\overrightarrow{\Delta E} \times \vec{B}$ spark plasma circulation drift rate

$$\hat{P}_3 = \frac{2\pi d}{\upsilon_d}$$

circumferential drift at the Polar Cap boundary

$$d \approx r_p = 1.4 (B_s / B_d)^{-1/2} 10^4 P^{1/2} \quad [\mathrm{cm}]$$

$$\upsilon_d = \frac{c\Delta E}{B_s} = \frac{c\eta(2\pi / cP)B_s h}{B_s} = \eta \frac{2\pi}{P} h \ \ [\mathrm{cm/s}]$$

B_s *-actual surface magnetic field*

B_d *-dipolar magnetic field at PC*

ΔE *- component of electric field caused by charge depletion* $\Delta\rho = \rho_{GJ} - \rho_{th} = \eta\rho_{GJ}$

Time interval to complete one circulation around periphery of PC

$$\hat{P}_3 = \frac{P}{2\eta} \frac{r_p}{h}$$

$\hat{P}_3 / P \sim 15 - 40$

$r_p / h \sim 5 - 10$

$\eta \sim 0.05 - 0.1$

Gil, Melikidze
& Geppert 2003

Within the *E x B* drift in PSG model we obtained interrelation between

L_x and $\hat{P}_3$ that does not depend on any details of the gap $h, b, \eta, \Re$

Thermal X-ray luminosity from spark-heated polar cap

$$L_x = 2.9 \times 10^{31} \times (\dot{P}_{-15} / P^3)(\hat{P}_3 / P)^{-2} \text{ erg/s}$$

Efficiency

$$L_x / \dot{E} = 0.75 (\hat{P}_3 / P)^{-2}$$

$$\dot{E} = I \Omega \dot{\Omega}$$

Spin-down power

$$T_s = (5.1 \times 10^6 K)(B_s / B_d)^{0.25} (\dot{P}_{-15})^{-0.5} P^{-0.5} (\hat{P}_3 / P)^{-0.5}$$

Surface temperature of PC

Polar cap radius and surface area

Locus of the open magnetic field lines

$$r_{pc} = 1.45 \times 10^{4} P^{-0.5}\ cm$$

Canonical radius

$$r_p = b^{-0.5} r_{pc}$$

Actual value

$$\boxed{b = B_s / B_d = A_{pc} / A_p = A_{pc} / A_{bol}}$$

B_s **Actual field**

B_d **Dipolar field**

$$A_{pc} = \pi r_{pc}^2$$

canonical

Surface area

bolometric

$$A_p = \pi r_p^2 = b^{-1} A_{pc}$$

XMM-Newton observations of drifting subpuslse PSR 0943+10

(Zhang, Sanwal & Pavlov 2005)

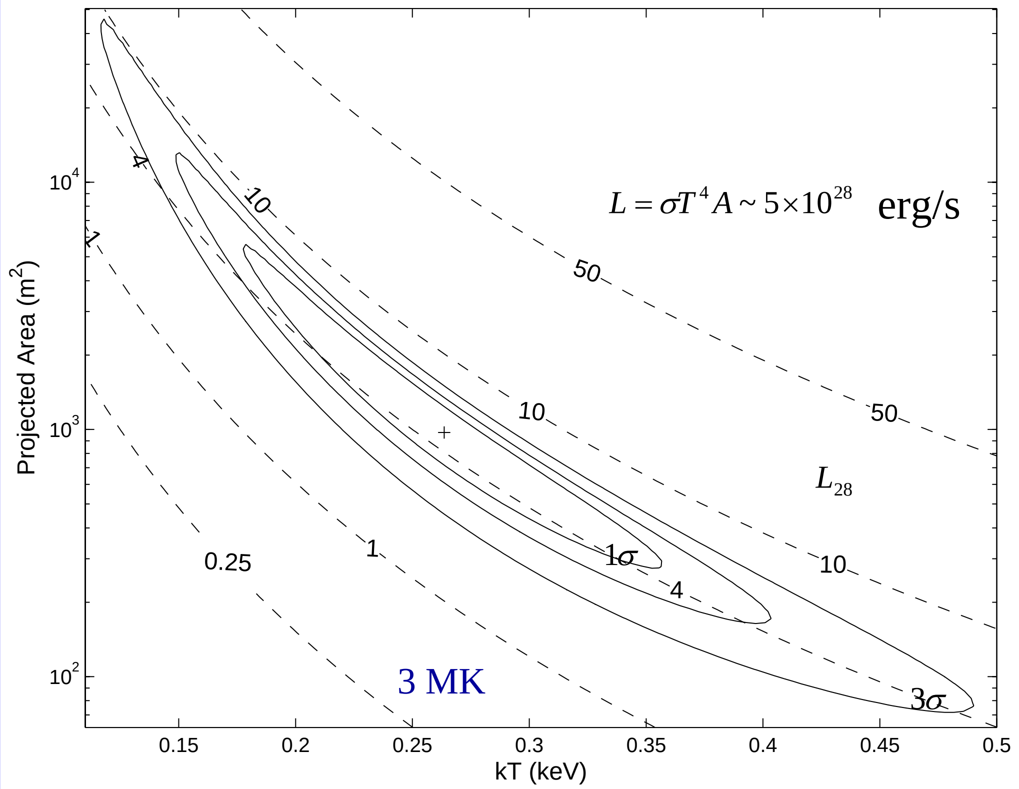

Consistent with thermal radiation from hot polar cap

Best BB fit:

A = 10^3(T/3MK)$^{-4}$ m^2

= (300 – 5000) m^2 ~1000 m^2

$A_{RS} = 6\times10^4$ m^2

T = (2.0-4.2) MK

$$L = \sigma T^4 A \sim 5\times10^{28} \text{erg/s}$$

68% confidence

$A << A_{RS}$

typical for thermal radiation from hot spots detected in a number of X-ray pulsars

B0943+10

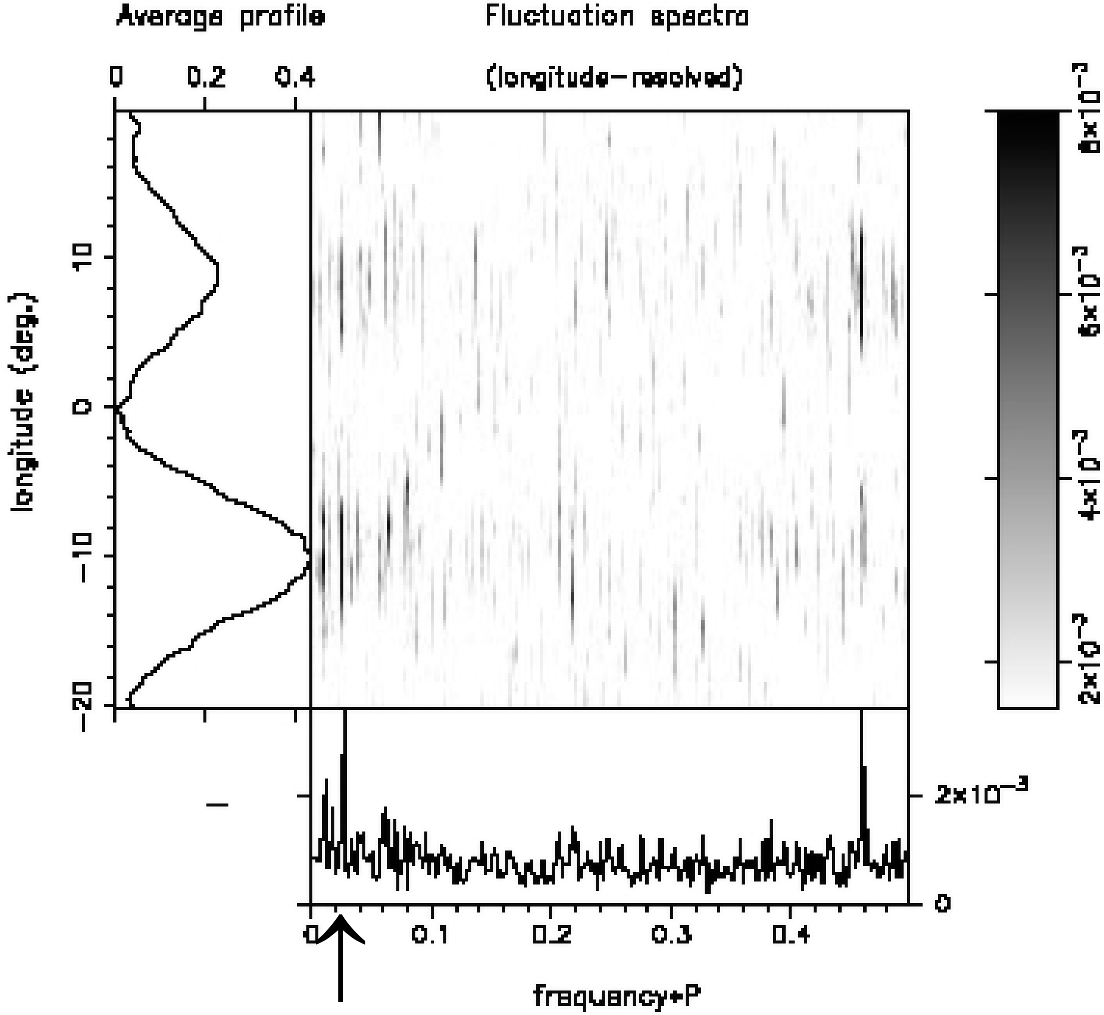

1/37

Deshpande
Rankin
Asgekar
1999,2001,2005

$$\hat{P}_3 / P \sim 37$$

Gil, Melikidze & Zhang 2006

$$\eta = (1/2\pi)(P/P_3)$$

Screening factor ~(0.05-0.1)

only few % of GJ plasma involved in acceleration

$$L_x = 2.9 \times 10^{31} \times (\dot{P}_{-15}/P^3)(\hat{P}_3/P)^{-2} \quad \text{erg/s}$$

X-ray luminosity

$10^{(28-29)}$ erg/s

$$L_x / \dot{E} = 0.75(\hat{P}_3/P)^{-2}$$

Efficiency ~ 0.001

Name	$\hat{P}_3/P$		$L_x/\dot{E} \times 10^{-3}$		$L_x \times 10^{28}$		b	$T_s^{(obs)}$	$T_s^{(pred)}$	B_d	B_s
PSR B	Obs.	Pred.	Obs.	Pred.	Obs.	Pred.	A_{pc}/A_{bol}	10^6 K	10^6 K	10^{12}G	10^{14}G
0943 + 10	37.4	37	$0.5^{+0.2}_{-0.2}$	0.46	5^{+2}_{-2}	4.8	60^{+140}_{-48}	$3.1^{+0.9}_{-1.1}$	3^{+1}_{-1}	3.95	$2.37^{+5.53}_{-1.90}$
1133 + 16	(33^{+3}_{-3})	31^{+3}_{-2}	$0.77^{+0.13}_{-0.18}$	$1.0^{+0.3}_{-0.2}$	$7.7^{+1.3}_{-1.3}$	$8.9^{+1.3}_{-1.8}$	$11.1^{+16.6}_{-5.6}$	$2.8^{+1.2}_{-1.2}$	$2.4^{+0.8}_{-0.5}$	4.25	$0.47^{+0.71}_{-0.24}$

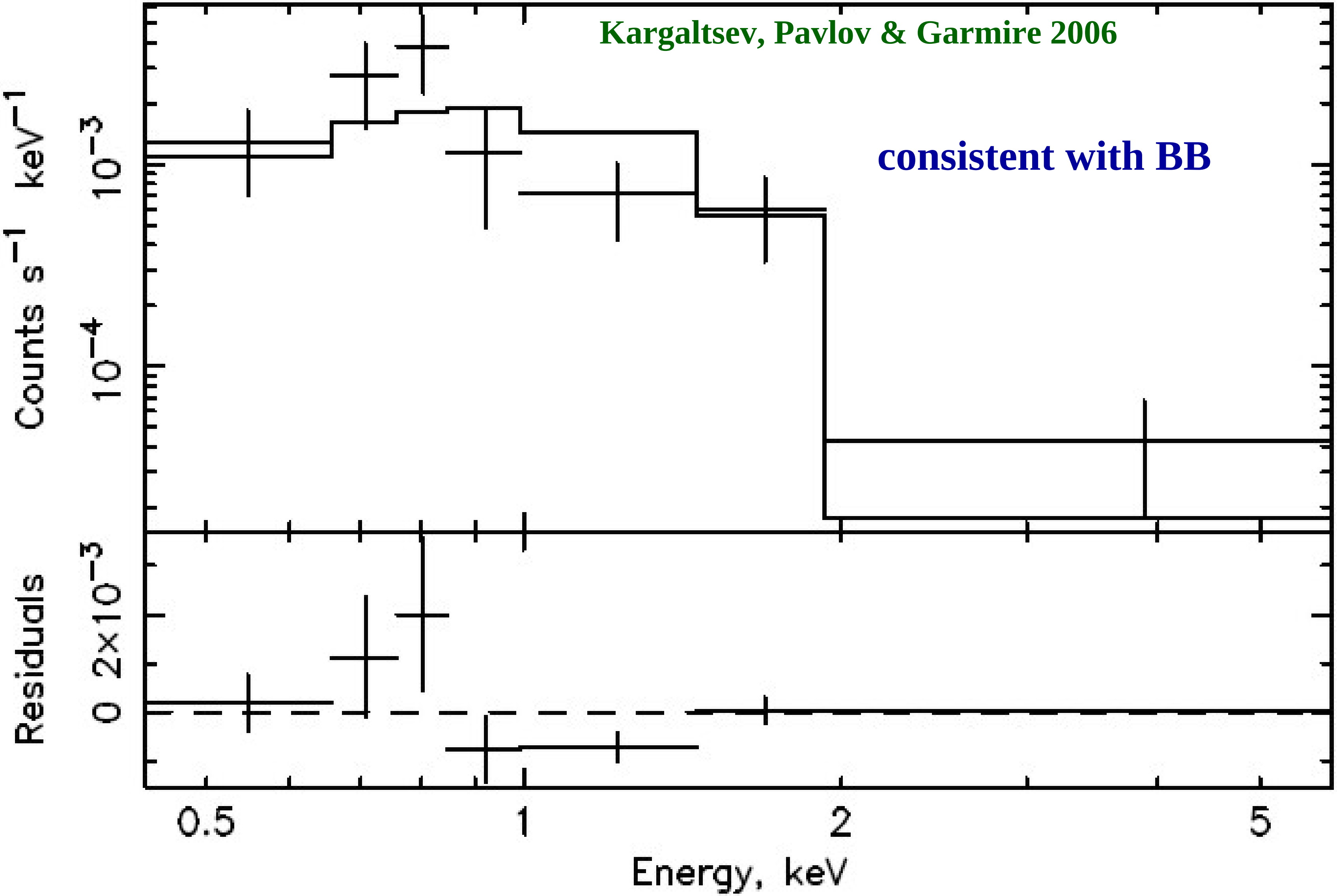

XMM-Newton spectrum of PSR B1133+16

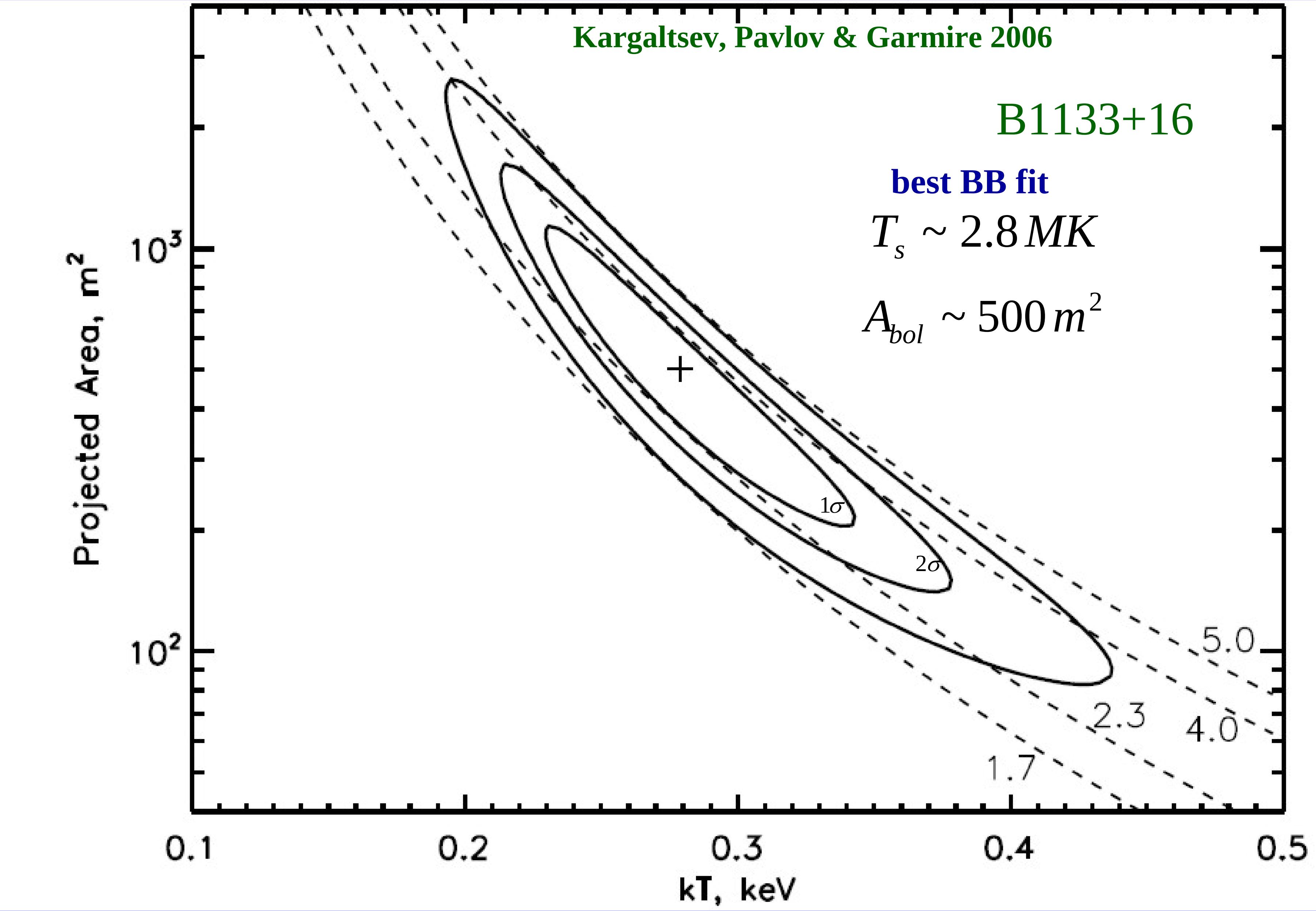

Kargaltsev, Pavlov & Garmire 2006
B1133+16
best BB fit
$T_s \sim 2.8\,MK$
$A_{bol} \sim 500\,m^2$
Projected Area, m²
10³
10²
kT, keV
0.1
0.2
0.3
0.4
0.5
1σ
2σ
5.0
4.0
2.3
1.7

Nowakowski, L., 1996, ApJ, 457,868

Weltevrede, Edwards And Stappers,. 2006

Fluctuation spectrum of PSR B1133+16

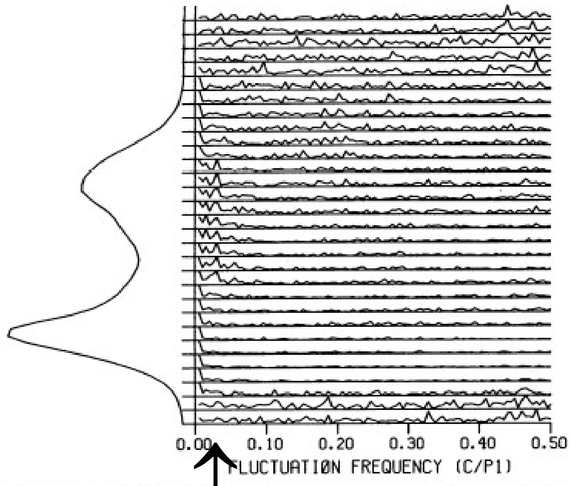

FIG. 10.—Longitude-resolved, unsmoothed power spectrum of PSR 1133 + 16 at 430 MHz. Thirty subwindows cover slightly more than the pulse window. Each power spectrum is individually normalized.

Single pulses

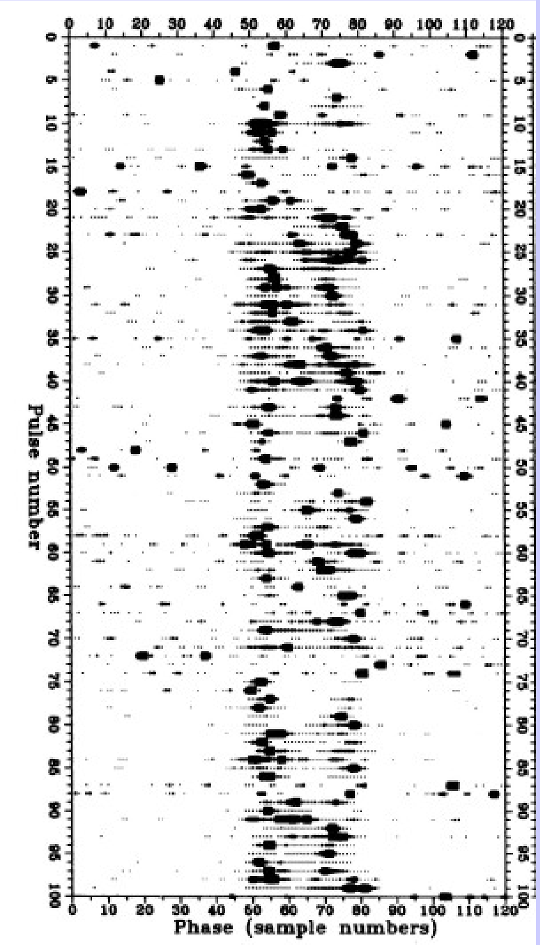

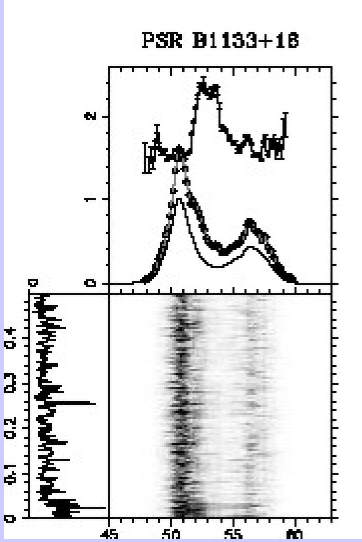

← *0.03 c/P*

33 ± 3

Long period feature

0.031c/P => 32P

$\hat{P}_3 / P = 32$?

YES

Name	$\hat{P}_3/P$		$L_x/\dot{E}\times10^{-3}$		$L_x\times10^{28}$		b	$T_s^{(obs)}$	$T_s^{(pred)}$	B_d	B_s
PSR B	Obs.	Pred.	Obs.	Pred.	Obs.	Pred.	A_{pc}/A_{bol}	10^6 K	10^6 K	10^{12}G	10^{14}G
$0943+10$	37.4	37	$0.5^{+0.2}_{-0.2}$	0.46	5^{+2}_{-2}	4.8	60^{+140}_{-48}	$3.1^{+0.9}_{-1.1}$	3^{+1}_{-1}	3.95	$2.37^{+5.53}_{-1.90}$
$1133+16$	(33^{+3})	31^{+3}	$0.77^{+0.13}$	$1.0^{+0.3}$	$7.7^{+1.3}$	$8.9^{+1.3}$	$11.1^{+16.6}$	$2.8^{+1.2}$	$2.4^{+0.8}$	4.25	$0.47^{+0.71}$

The only two cases existing with both measurements

B1133+16 $L_x/\dot{E} \sim 0.77\times10^{-3}$ $\hat{P}_3/P \sim 33$

B0943+10 $L_x/\dot{E} \sim 0.5\times10^{-3}$ $\hat{P}_3/P \sim 37$

Future work

New XMM-Newton observations of PSR B0826-34 planned this fall – 50 Ks proposal granted
Zhang, Gil, Melikidze, Geppert, Haberl

$$\hat{P}_3 / P = 15$$

(Gupta, Gil, Kijak et al. 2004)

Proposal for XMM-Newton observations of PSR B0834+06 will be submitted for the next cycle

$$\hat{P}_3 / P = 15$$

(Asgekar, Deshapande 2005)

MPIfR - Bonn Pulsar Group

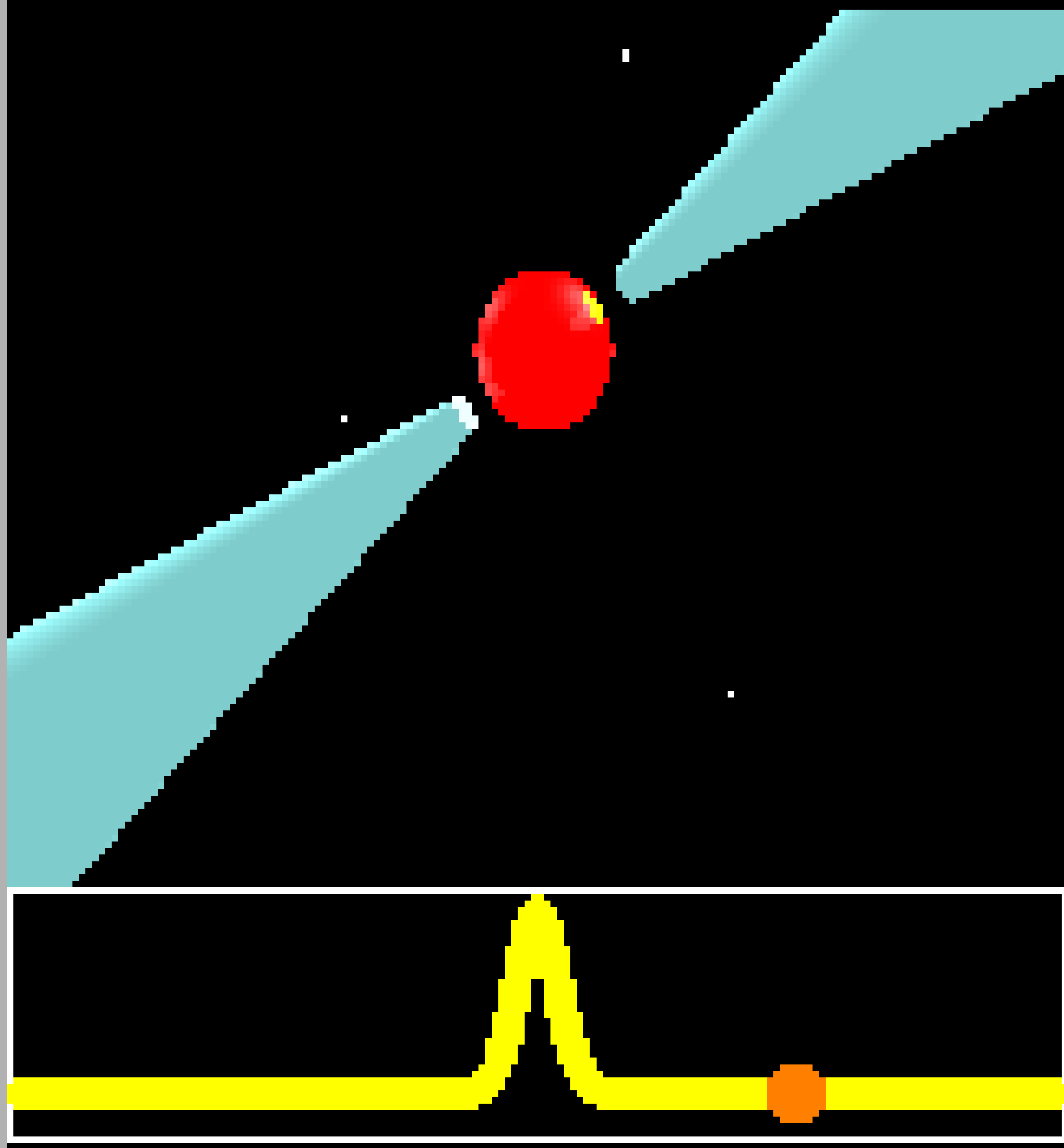

Termoregulation of PSG

Backflowing bombardment associated with spark plasma development heats the PC surface to temperatures lower than critical temperature (above which there is free flow).

The higher the temperature the more intense thermionic emission, which in turn means more screening and less intense heating.

This thermolegulation should establish the quasi-steady state at temperature very close (but slightly lower) to the critical temperature

$$T_s \cong T_i$$

Weltevrede, Edwards & Stappers 2006

Unbiased search for drifting subpulses in 186 pulsars

~1300 pulsars •

Common phenomenon

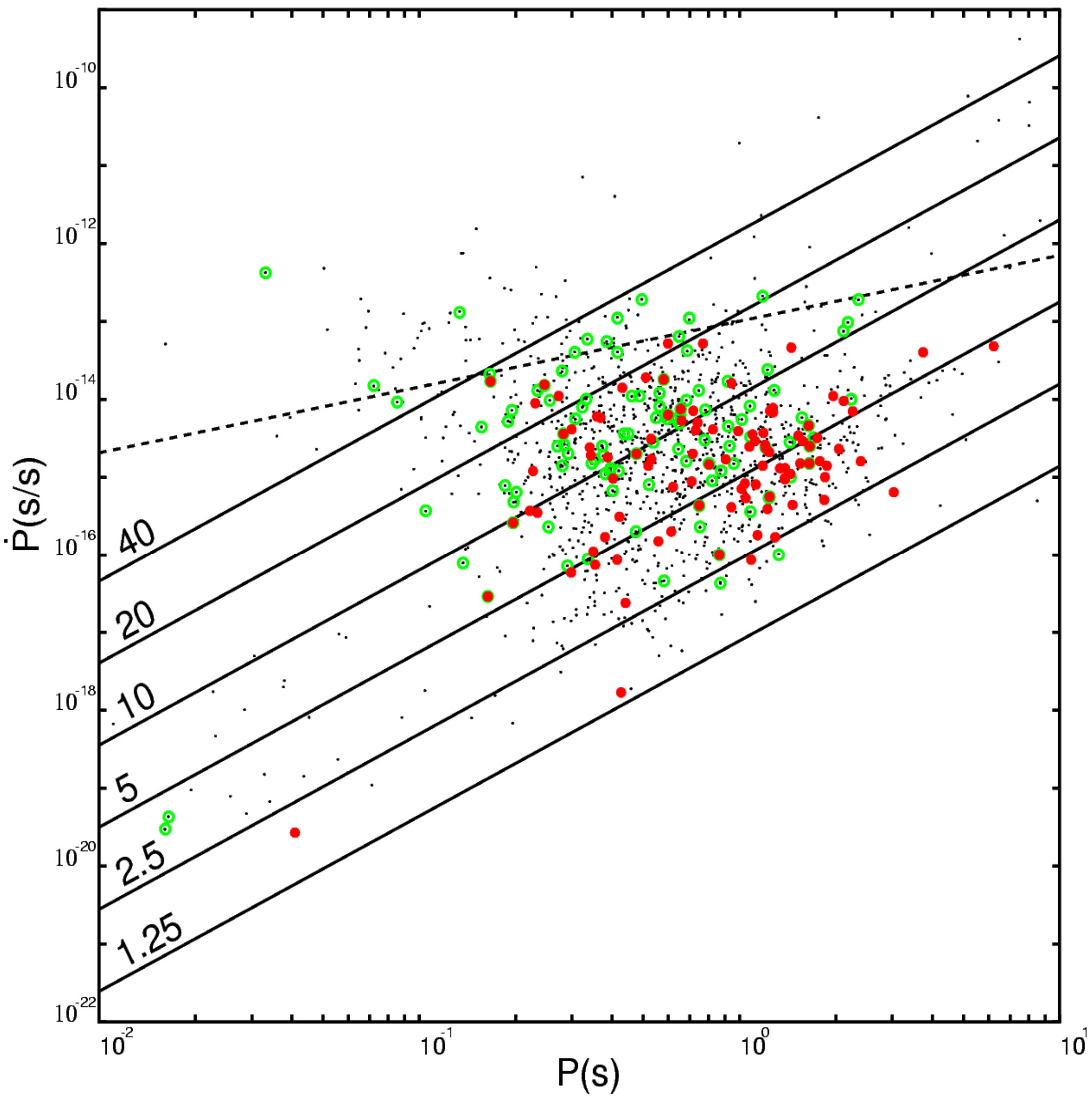

~106

PSRs with detected drifting subpulses *

more than 55 %

Drifting subpulses not detected *
very poor S/N

Polar gap model of B0943+10 consistent with XMM-Newton

(Gil, Melikidze & Geppert 2003, Zhang, Sanwal & Pavlov 2005; Gil, Melikidze & Zhang 2006)

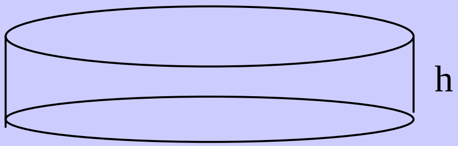

Pure VG – too luminous in X-ray
SCLF – too dim in X-ray

Partially screened gap gives
- right bolometric area $A = 10^7\ cm^2$
- right surface temperature T~3 MK
- right drift periodicity $\hat{P}_3 / P \sim 37$

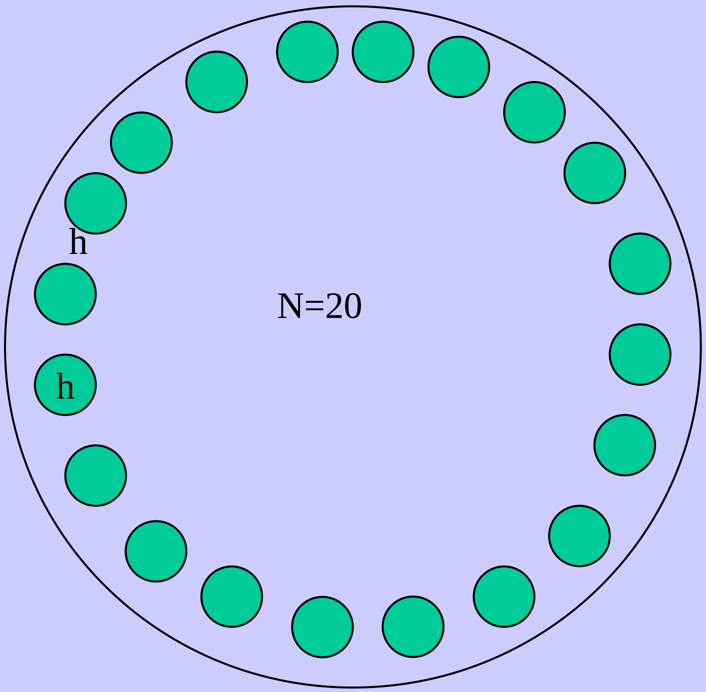

Characteristic spark dimension ~ h

Sparking discharge of charge depleted acceleration region

Potential drop $10^{11-12}V$ exceeds threshold for the magnetic pair production – cascade developes until corotational charge is rebuild – this restores corotation for short time *t~h/c~(10-100)ns*

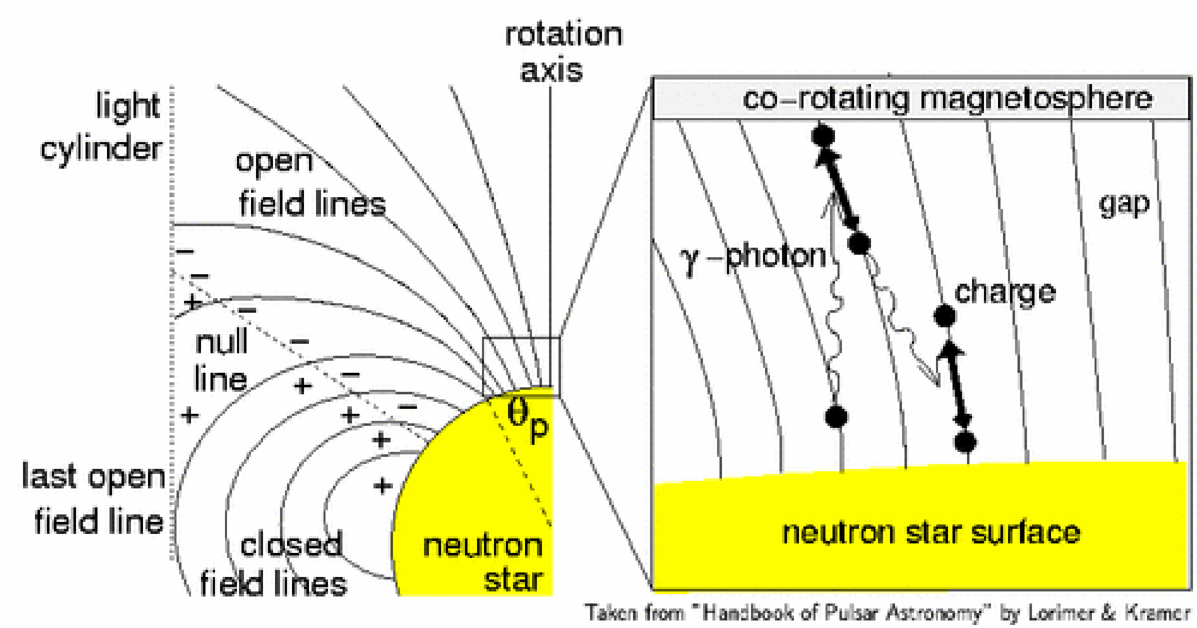

$\Delta V(h)$

h

Gap height *h* determined by the mean free path of photons for the magnetic pair production. The accelerating potential drop

$$\Delta Ve = \frac{2\pi e}{cP} B_s h^2 \sim 10^6 MeV$$

Inner acceleration region and structure of surface magnetic field B_s

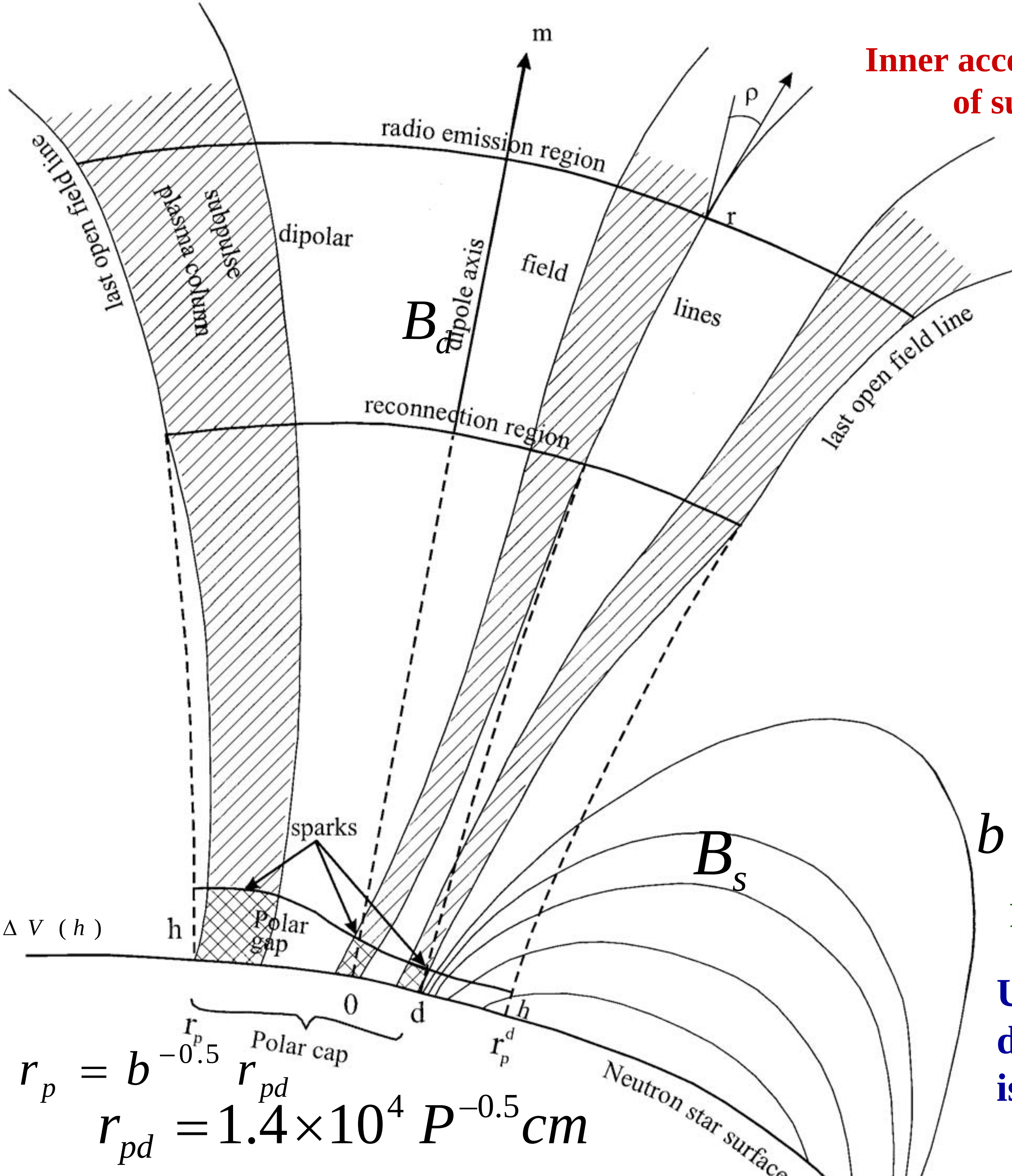

$$r_p = b^{-0.5} r_{pd}$$

$$r_{pd} = 1.4 \times 10^4 P^{-0.5} cm$$

Assume:

Strong non-dipolar surface magnetic field

Consistent with:

Spectral lines

Small bolometric PC areas compared with canonical values

$$b = B_s / B_d = A_{pc} / A_{bol}$$

Ruderman & Sutherland 1975

Ultra-high gap potential drop discharges via a number of isolated spark filaments

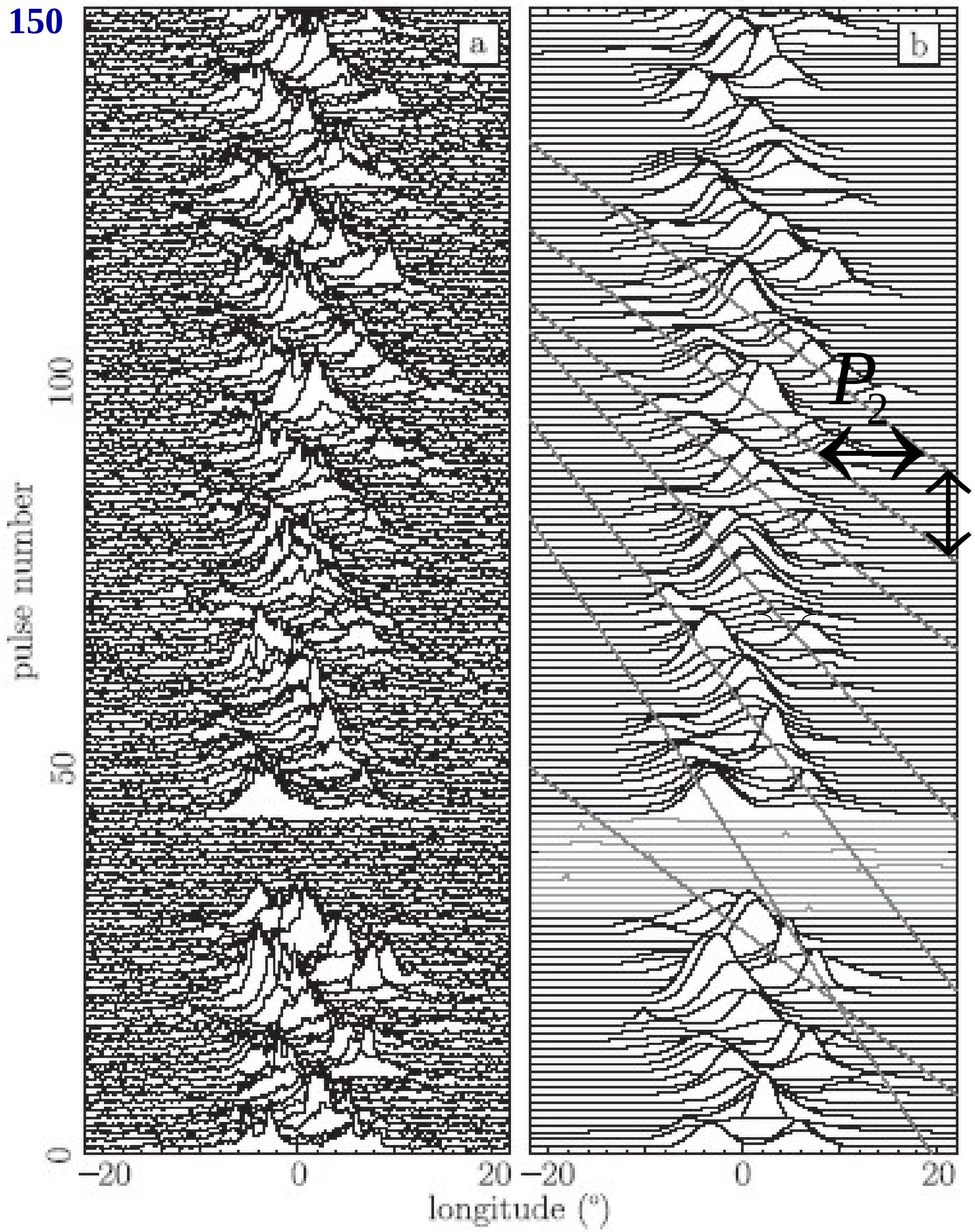

PSR B0809+74

Sequence of 150 single pulses folded at pulsar basic period $P = 1.29\,s$

Apparent subpulse drift-bands

$P_3 \approx 11P$

Modulation of intensity along drift-bands consistent with carousel model

apparently

Sub-beams continue to circulate beyond the observed pulse-window

(after van Leuven, Stappers et al..)

Co-rotating magnetosphere

$$E_c = -(\Omega \times r / c) \times B_s$$

Force-free magnetosphere

$$E_c \cdot B_s = 0$$

$$\Delta V_{\parallel} = 0$$

No acceleration along *B*

GJ69, RS75

$$\rho_c = (1/2\pi)\, div E_c =$$

$$= -\Omega \cdot B_s /(2\pi c) = \pm B_s / cP$$

Co-rotating charge density

$$\upsilon_{cor} = c(E_c \times B_s)/B^2 = cE_c / B_s$$

Linear co-rotation velocity

Possible interrelation between radio and X-ray signatures of drifting subpulses in pulsars

L_x **versus** $\hat{P}_3$

Thermal luminosity from polar cap heated by sparks associated with (drifting) subpulses

$$L_x = \sigma T_s^4 A_{bol} = \sigma T_s^4 A_{pc} (B_s / B_d)$$

Tertiary subpulse drift periodicity → circulation period of subpulse associated sparks

$$\hat{P}_3 \approx 2\pi r_p / \upsilon_d = 2\pi r_{pc} (B_s / B_d) / \upsilon_d$$

101 pulsars with detected drifting subpulses

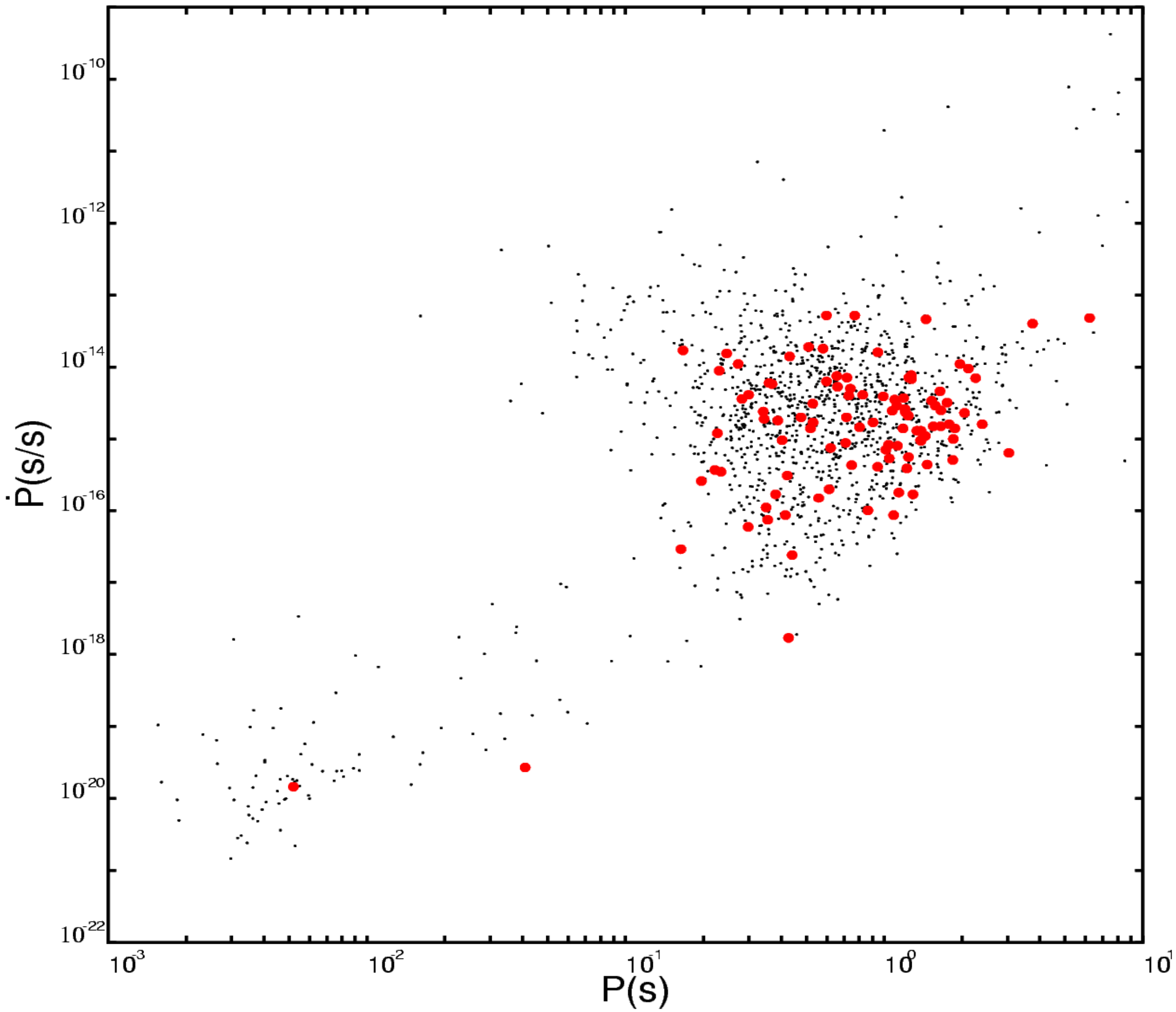

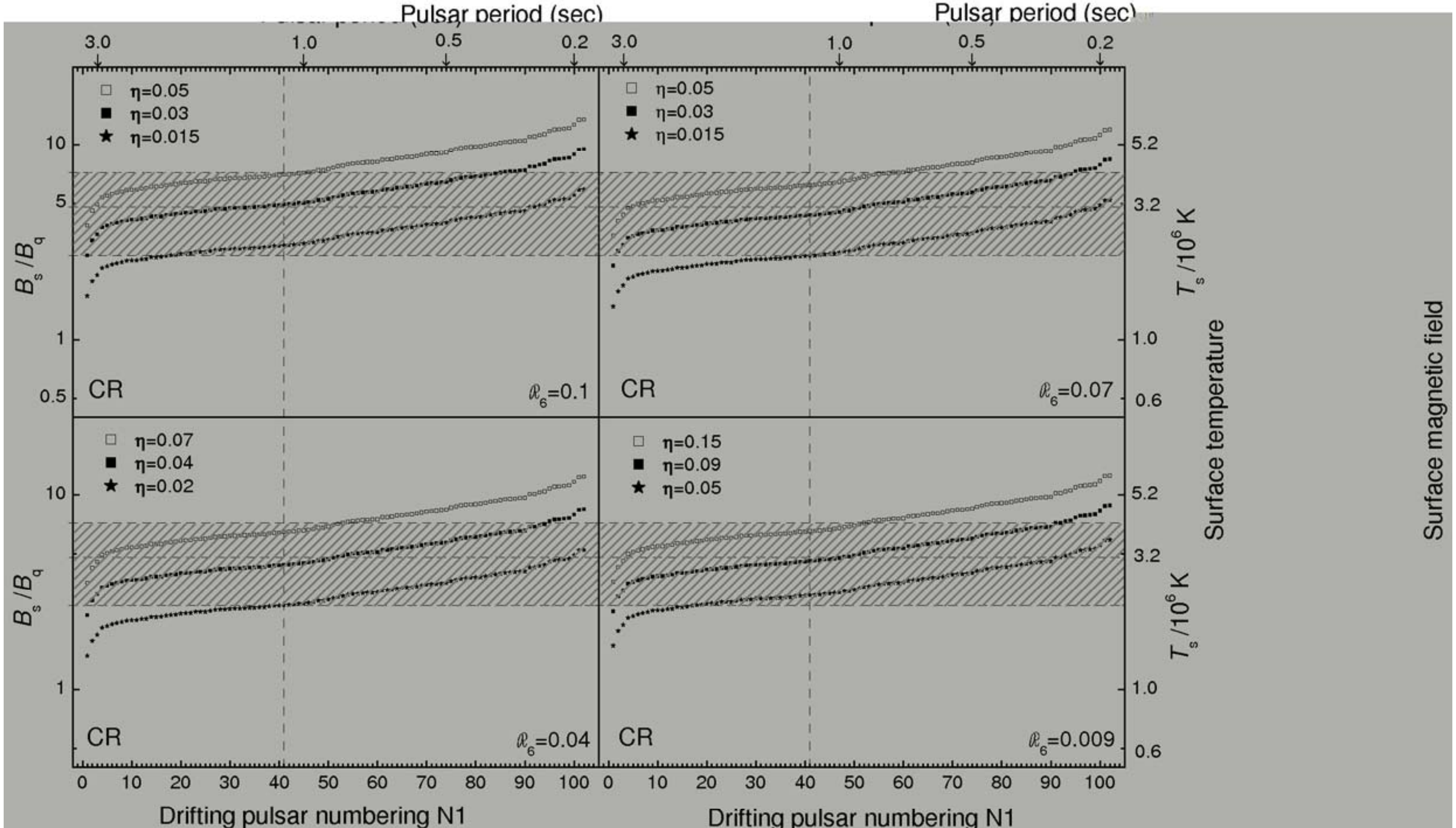

Pulsar period (sec)
3.0
1.0
0.5
0.2
η=0.05
η=0.03
η=0.015
η=0.07
η=0.04
η=0.02
η=0.15
η=0.09
η=0.05
CR
$\mathcal{R}_6$=0.1
$\mathcal{R}_6$=0.07
$\mathcal{R}_6$=0.04
$\mathcal{R}_6$=0.009
B_s/B_q
$T_s/10^6$ K
Surface temperature
Surface magnetic field
Drifting pulsar numbering N1

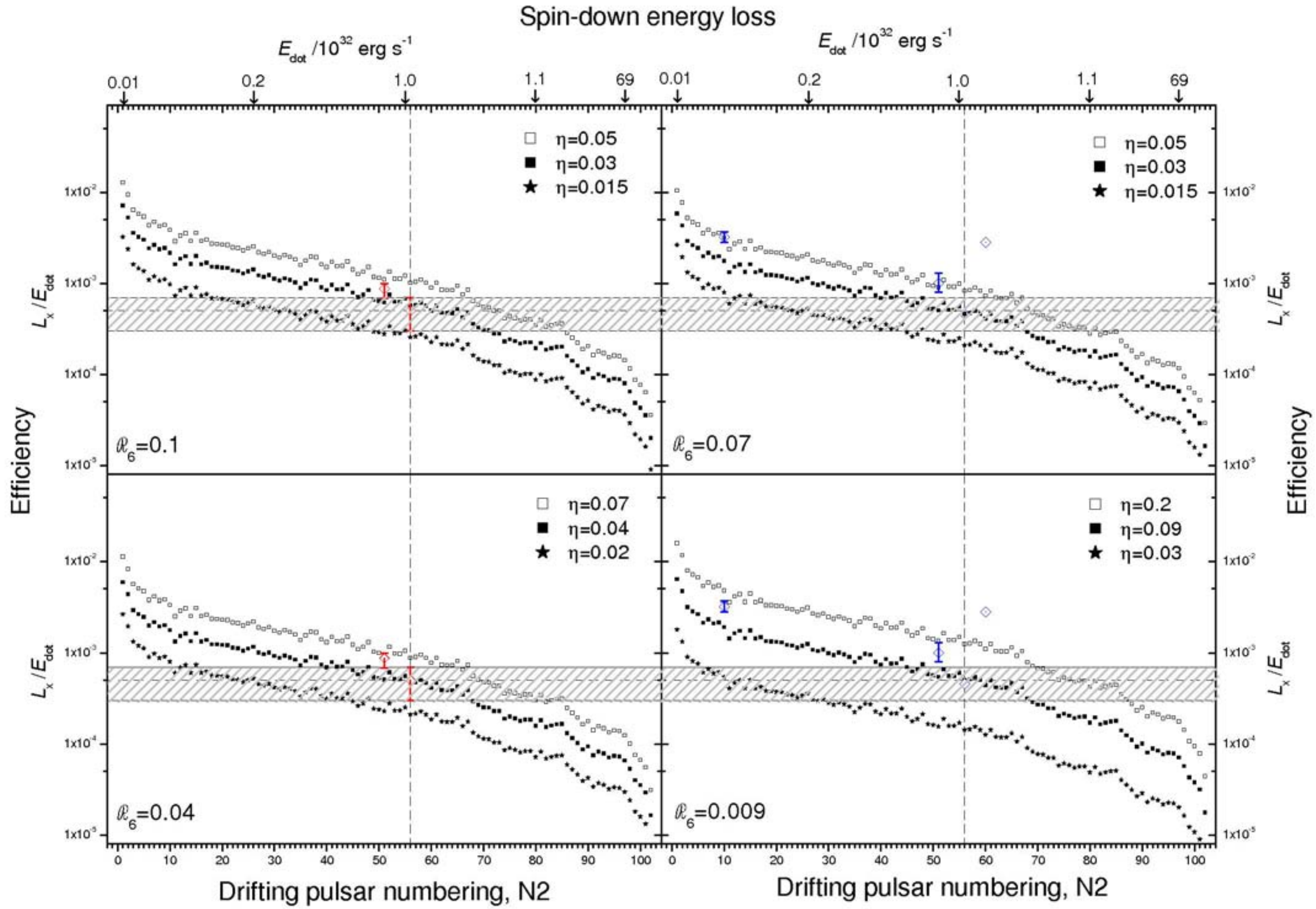

Spin-down energy loss
E_{dot} /10^{32} erg s^{-1}
0.01
0.2
1.0
1.1
69
η=0.05
η=0.03
η=0.015
η=0.07
η=0.04
η=0.02
η=0.2
η=0.09
η=0.03
$\mathcal{R}_6$=0.1
$\mathcal{R}_6$=0.07
$\mathcal{R}_6$=0.04
$\mathcal{R}_6$=0.009
Efficiency
L_x /E_{dot}
1x10^{-2}
1x10^{-3}
1x10^{-4}
1x10^{-5}
Drifting pulsar numbering, N2

Internal structure of the pulsar beam reflected in complex shapes of single pulses and/or mean profiles (some degree of symmetry in profiles) (correlations with the impact angle)

Nested cones

Patches

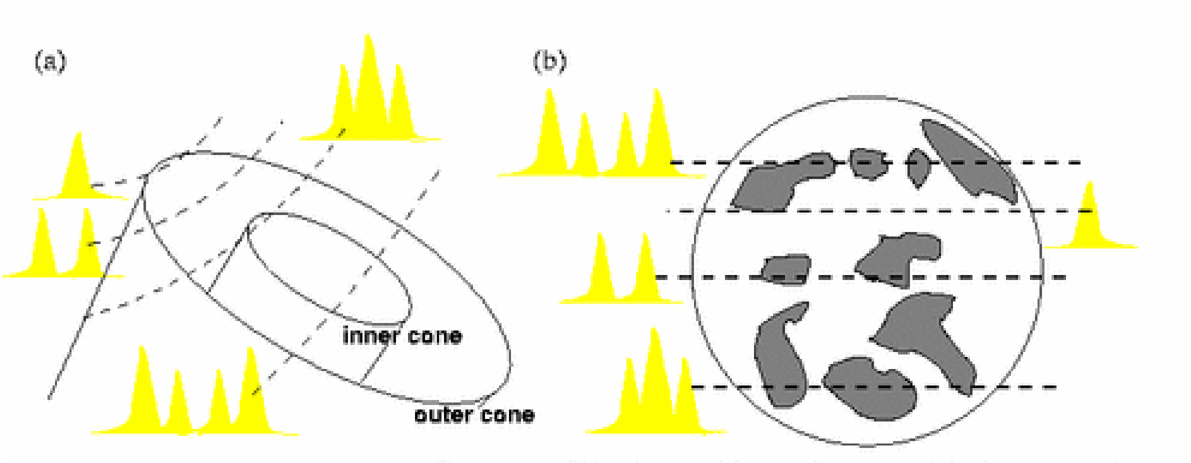

Taken from "Handbook of Pulsar Astronomy" by Lorimer & Kramer

Rankin 1993, Gil et al. 1993

Lyne & Manchester 1988

P0834+06 1404 MHz

Central cut

Longitude stationary even-odd intensity modulation
different manifestation of the same phenomenon

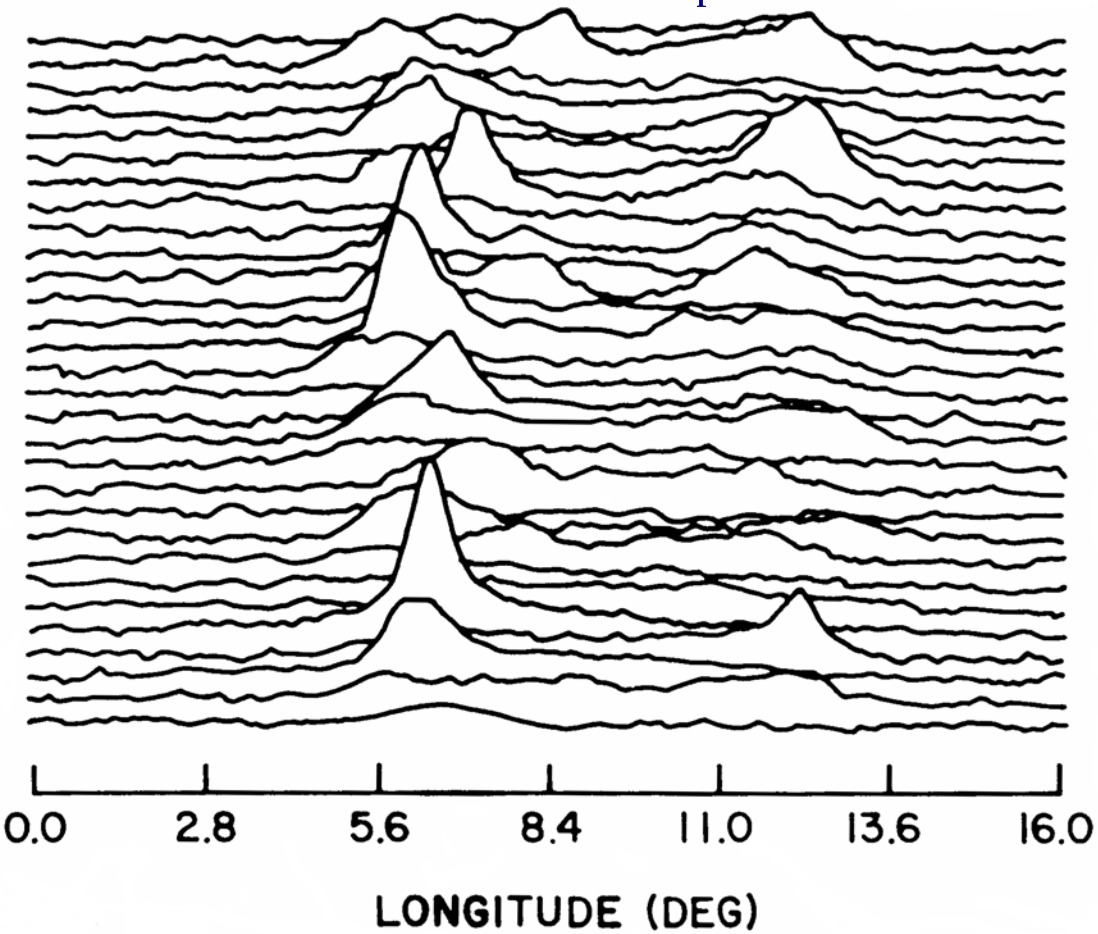

Rotating sub-beams cut the line-of-sight in phases corresponding to the component peaks

drift visible in the saddle as well

l-of-s cuts more central

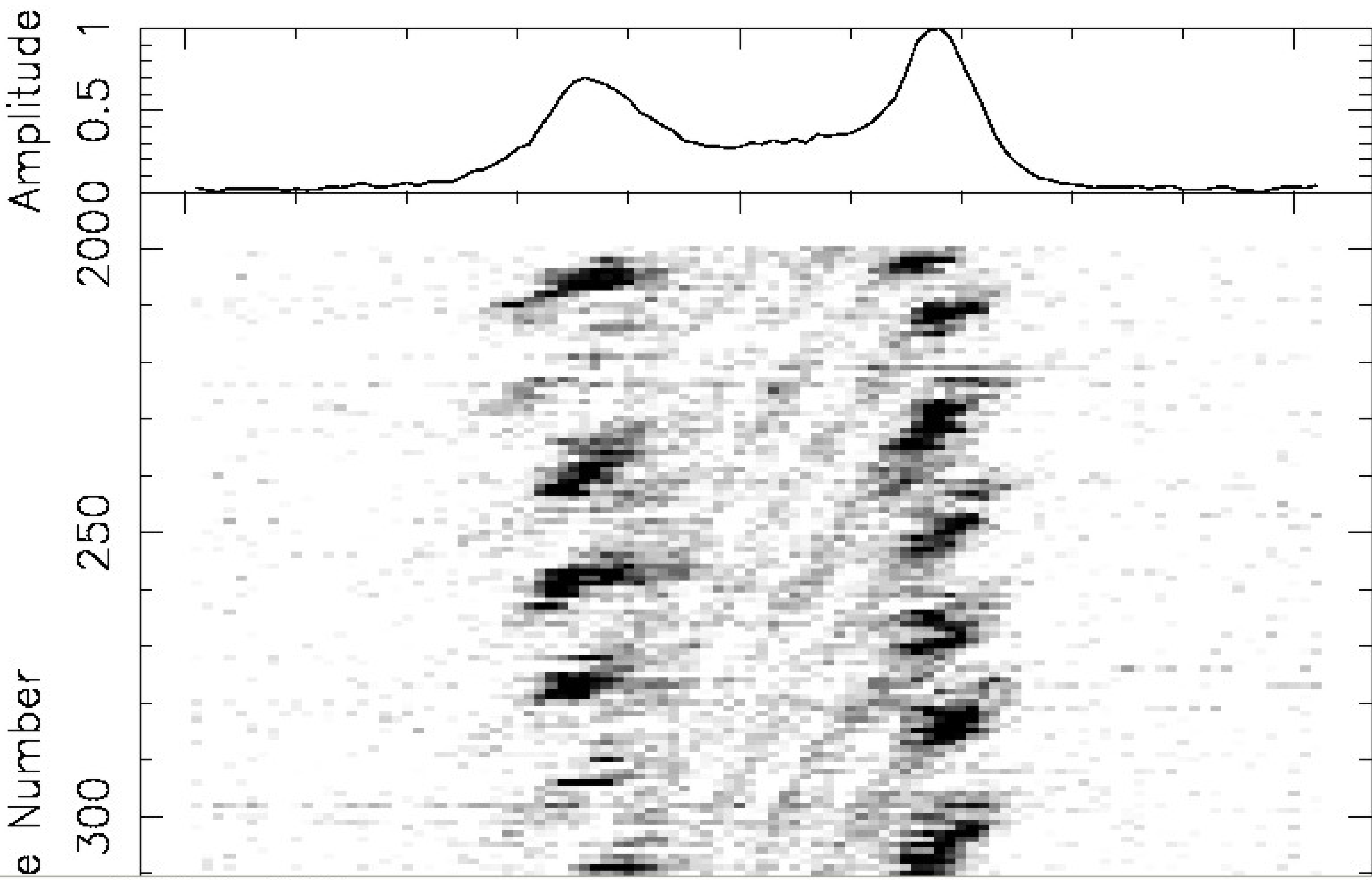

Rotating, magnetized Neutron Star

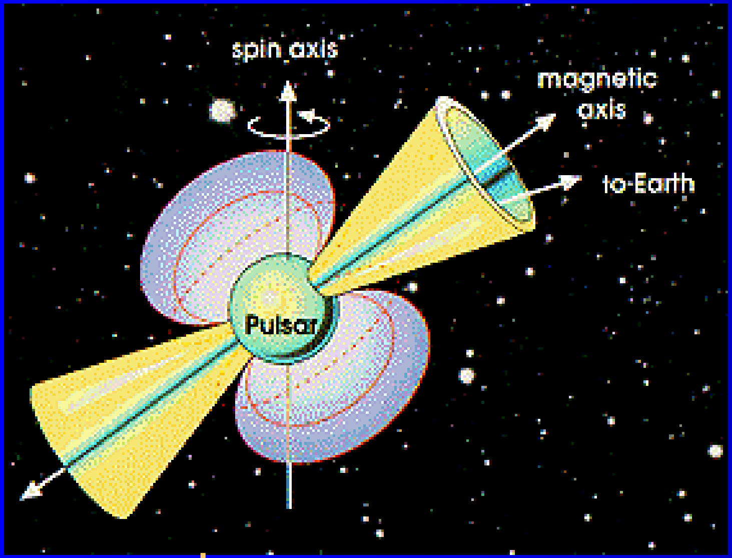

Pulsar

Internal beam structure

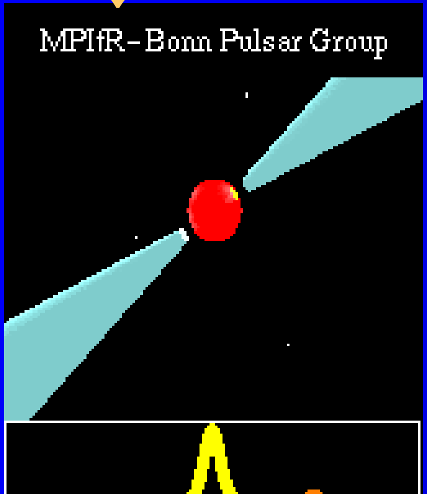

Complex pulse shapes